Transcriptomic and Reverse Genetic Analyses of Branched-Chain Fatty Acid and Acyl Sugar Production in *Solanum pennellii* and *Nicotiana benthamiana*[1][W][OA]

Stephen P. Slocombe, Ines Schauvinhold[2], Ryan P. McQuinn[3], Katrin Besser, Nicholas A. Welsby[4], Andrea Harper[5], Naveed Aziz, Yi Li, Tony R. Larson, James Giovannoni[3], Richard A. Dixon[6], and Pierre Broun[7]*

Department of Biology, Area 7, University of York, York YO10 5YW, United Kingdom

Acyl sugars containing branched-chain fatty acids (BCFAs) are exuded by glandular trichomes of many species in Solanaceae, having an important defensive role against insects. From isotope-feeding studies, two modes of BCFA elongation have been proposed: (1) fatty acid synthase-mediated two-carbon elongation in the high acyl sugar-producing tomato species *Solanum pennellii* and *Datura metel*; and (2) α-keto acid elongation-mediated one-carbon increments in several tobacco (*Nicotiana*) species and a *Petunia* species. To investigate the molecular mechanisms underlying BCFAs and acyl sugar production in trichomes, we have taken a comparative genomic approach to identify critical enzymatic steps followed by gene silencing and metabolite analysis in *S. pennellii* and *Nicotiana benthamiana*. Our study verified the existence of distinct mechanisms of acyl sugar synthesis in Solanaceae. From microarray analyses, genes associated with α-keto acid elongation were found to be among the most strongly expressed in *N. benthamiana* trichomes only, supporting this model in tobacco species. Genes encoding components of the branched-chain keto-acid dehydrogenase complex were expressed at particularly high levels in trichomes of both species, and we show using virus-induced gene silencing that they are required for BCFA production in both cases and for acyl sugar synthesis in *N. benthamiana*. Functional analysis by down-regulation of specific *KAS I* genes and cerulenin inhibition indicated the involvement of the fatty acid synthase complex in BCFA production in *S. pennellii*. In summary, our study highlights both conserved and divergent mechanisms in the production of important defense compounds in Solanaceae and defines potential targets for engineering acyl sugar production in plants for improved pest tolerance.

Glandular trichomes are epidermal secretory structures that play a central defensive role in many plant species. Due to their unique and versatile metabolism, they contribute significantly to the wide diversity of phytochemicals. Some trichome types produce acyl sugars, which are nonvolatile metabolites that are exuded onto the surface of aerial organs. These highly viscous lipids constitute a significant proportion of leaf biomass in the Solanaceae and are produced in particularly large amounts in the wild tomato species *Solanum pennellii* (up to 20% leaf dry weight; Fobes et al., 1985). Certain wild tobacco (*Nicotiana*) species produce up to 15% leaf dry weight (G. Wagner, personal communication), and they are also produced, albeit in lesser quantities, in the model tobacco species *Nicotiana benthamiana* (Shinozaki et al., 1991; Ohya et al., 1994; Kroumova and Wagner, 2003). Due to the potent antifeedant, antioviposition, and in some cases toxic properties of these compounds in relation to insect pests, increasing acyl sugar production has long been a target of tomato and potato (*Solanum tuberosum*) breeding programs (Bonierbale et al., 1994; Chortyk, 1997; Lawson et al., 1997; Mutschler et al., 2001; McKenzie et al., 2005). Many acyl sugars tested have insecticidal and miticidal activity exceeding the efficiency of a comparable standard, insecticidal soap (Puterka et al., 2003). Trichome-derived acyl sugars have also been recognized for their potential as alternatives to chemically synthesized food-grade Suc esters, as antibiotics, and for cosmetic applications (Chortyk et al., 1993; Hill and Rhode, 1999). However,

[1] This work was supported by the Samuel Roberts Noble Foundation and the National Science Foundation (grant no. 0605033).

[2] Present address: Molecular, Cellular, and Developmental Biology, University of Michigan, 830 North University, Ann Arbor, MI 48109.

[3] Present address: U.S. Department of Agriculture-Agricultural Research Service and Boyce Thompson Institute for Plant Research, Tower Road, Cornell University, Ithaca, NY 14853.

[4] Present address: Physiology Laboratory, Downing Street, Cambridge CB2 3EG, United Kingdom.

[5] Present address: School of Biosciences, University of Birmingham, Edgbaston, Birmingham B15 2TT, United Kingdom.

[6] Present address: Samuel Roberts Noble Foundation, 2510 Sam Noble Parkway, Ardmore, OK 73401.

[7] Present address: Nestlé R&D Center Tours, Plant Science and Technology, 101 Avenue G. Eiffel, 37390 Notre Dame d'Oé, France.

* Corresponding author; e-mail pierre.broun@rdto.nestle.com.

The author responsible for distribution of materials integral to the findings presented in this article in accordance with the policy described in the Instructions for Authors (www.plantphysiol.org) is: Pierre Broun (pierre.broun@rdto.nestle.com).

[W] The online version of this article contains Web-only data.

[OA] Open Access articles can be viewed online without a subscription.

www.plantphysiol.org/cgi/doi/10.1104/pp.108.129510

a more complete understanding of the mechanism of acyl sugar synthesis and its regulation is necessary to increase their potential for further exploitation in plants.

Detached trichomes (heads and stalks) have been demonstrated to be capable of acyl sugar synthesis in *N. benthamiana* (Kroumova and Wagner, 2003). Glandular head cells alone have proven sufficient in *Nicotiana tabacum*, whereas epidermal strips with trichomes removed failed to synthesize acyl sugars (Kandra and Wagner, 1988). Periclinal grafting experiments and isotopic labeling studies using epidermal strips (with trichomes attached) indicate that the epidermal layer suffices for acyl sugar production in *S. pennellii* (Goffreda et al., 1990; Kroumova and Wagner, 2003). Direct demonstration of synthesis in detached trichomes of *S. pennellii* has not been shown, although this is considered to be the likely site of synthesis (Wagner, 1991; Kroumova and Wagner, 2003).

Plant acyl sugars are typically Glc or Suc esters that often contain branched-chain fatty acids (BCFAs; Severson et al., 1985; King and Calhoun, 1988; King et al., 1990). *S. pennellii* secretes a mix of Glc and Suc esters that contain predominantly BCFAs: 2-methylpropanoic acid (2MeC3:0), 2-methylbutanoic acid and 3-methylbutanoic acid (2MeC4:0 and 3MeC4:0), and 8-methylnonanoic acid (8MeC9:0), as well as some straight-chain fatty acids (SCFAs; C10:0 and C12:0; Burke et al., 1987; Shapiro et al., 1994; Li et al., 1999). In *N. benthamiana*, the predominant BCFAs are 6-methylheptanoic acid and 5-methylheptanoic acid (6MeC7:0 and 5MeC7:0), but the precise acyl sugar composition has not been described (Kroumova and Wagner, 2003).

A schematic illustration based on currently available information for our two model species of choice, *N. benthamiana* and *S. pennellii*, is shown (Fig. 1). Presumed pathways and fluxes for acyl sugar production in the two model species are shown with important caveats: (1) that intracellular targeting of the enzymes involved is assumed to be the same as for primary pathways of branched-chain amino acid (BCAA) synthesis and breakdown; (2) that plastid fatty acid synthase (FAS) is assumed to be the route for BCFA elongation in tomato; and (3) that it is not known if flux proceeds through amino acids or their immediate keto acid precursors. Production of Glc esters in *S. pennellii* involves glucosyltransferases with different fatty acid chain length specificities that add the first substituent to UDP-Glc, forming a β-1-*O*-acyl group (Ghangas and Steffens, 1995; Kuai et al., 1997). Further additions are catalyzed by an acyltransferase acting on Glc esters via a disproportionation reaction (Ghangas and Steffens, 1995; Li et al., 1999; Li and Steffens, 2000). This enzyme is glycosylated and synthesized with a cleavable signal peptide, indicating a probable endoplasmic reticulum location, thus suggesting a plausible route for acyl sugar export via a secretory vesicle pathway (Fig. 1; Li et al., 1999; Li and Steffens, 2000).

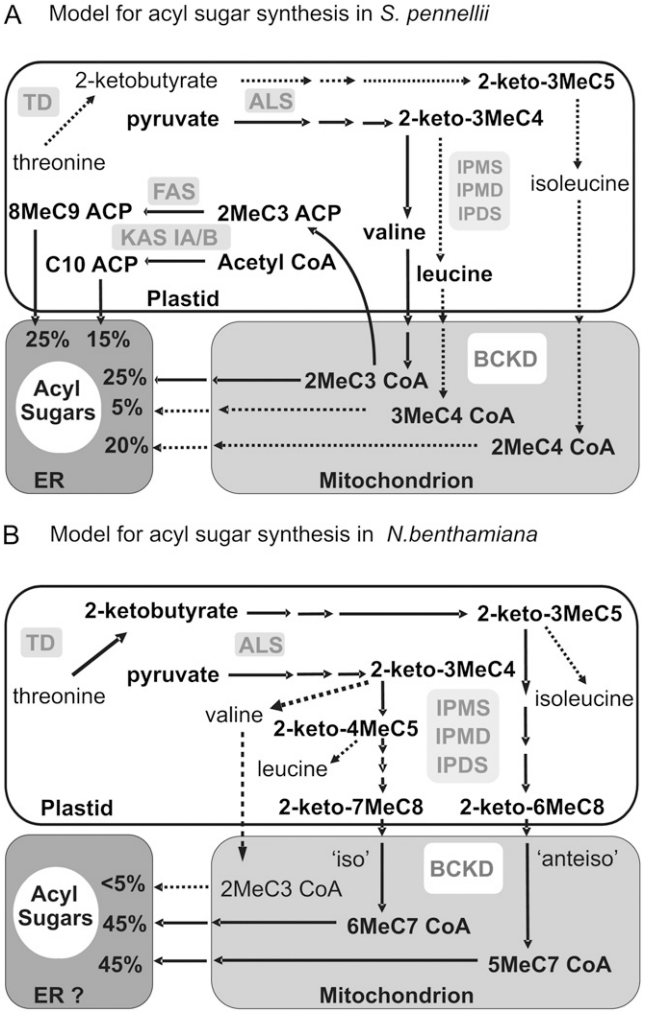

Figure 1. Proposed model of acyl sugar synthesis in *S. pennellii* (A) and *N. benthamiana* (B) assuming the same intracellular locations generally observed for primary metabolic pathways of BCAA synthesis and catabolism. Solid arrows and broken arrows depict major and minor metabolic routes, respectively, in acyl sugar formation deduced from chain composition. Proposed two-carbon elongation by plastidial FAS of BCFAs from a 2MeC3:0 precursor is shown for *S. pennellii* (A). Plausible operation of the *iso* and *anteiso* branches of the α-keto acid elongation pathway is shown for branched-chain elongation in *N. benthamiana* (B). EC numbers are as follows: TD (EC 4.2.1.16), ALS (EC 2.2.1.6), IPMS (EC 2.3.3.13), IPMD (EC 1.1.1.85), IPDS (EC 4.2.1.33), BCKD (EC 2.7.11.4), and KAS (EC 2.3.1.41). ER, Endoplasmic reticulum.

Inhibitor and feeding studies in *N. tabacum* and *S. pennellii* first suggested the plastid-located BCAA synthesis pathways as a source of keto acid precursors for acyl sugar chain synthesis (Fig. 1; Kandra et al., 1990; Kandra and Wagner, 1990; Walters and Steffens, 1990). Historically, two alternative mechanisms were put forward in these and later studies for the elongation of BCFAs (and SCFAs) destined for sugar esters in the Solanaceae (Kroumova et al., 1994; van der Hoeven and Steffens, 2000). Interestingly, evidence now suggests that different species within this family utilize

either one or the other of the two pathways (Kroumova and Wagner, 2003). In *S. pennellii* (and also later documented in *Datura metel*), short branched-chain acyl groups apparently act as primers for two-carbon elongation through the action of the FAS complex (Fig. 1A), a model that is supported by isotopic labeling studies (van der Hoeven and Steffens, 2000; Kroumova and Wagner, 2003). Contrasting with tomato and *Datura*, several tobacco species (including *N. benthamiana*) and *Petunia* species were shown by similar methodology to produce extended BCFAs (and also SCFAs in *Petunia*) via a one-carbon mechanism termed α-keto acid elongation (α-KAE; Fig. 1B; Kroumova et al., 1994; Kroumova and Wagner, 2003). Analogous to glucosinolate biosynthesis in Arabidopsis (*Arabidopsis thaliana*), this entails extended cycling through isopropyl malate synthase (IPMS), isopropyl malate dehydrogenase (IPMD), and isopropylmalate dehydratase (IPDS) to yield medium branched-chain keto acids. In primary metabolism, these steps are associated with Leu synthesis, but here choice of substrate is evidently wider (Kroumova and Wagner, 2003; Field et al., 2006). Interestingly, *iso-* and *anteiso*-branched chains are also significant components of wax alkanes, epicuticular esterified alcohols, and fatty acids in tobacco species, but according to isotope-labeling studies, the latter are generated by FAS-mediated elongation of branched-chain precursors rather than α-KAE (Kaneda, 1967; Kolattukudy, 1968; Kroumova and Wagner, 1999).

Elongation of BCFAs, either by FAS or α-KAE, raises interesting questions of substrate specificity and the need to identify specific genes. Furthermore, evidence to date has been based primarily on isotopic labeling studies with potential caveats indicated in the literature (van der Hoeven and Steffens, 2000; Kroumova and Wagner, 2003). This emphasizes the need for further investigation using genomic tools and gene functional analyses.

The branched-chain keto acid dehydrogenase (BCKD) step has long been proposed for the conversion of keto acids originating from α-KAE to acyl-CoAs, either for incorporation into acyl sugars or for potential entry into other pathways such as FAS (Kandra et al., 1990). In plants, BCKD is the first committed step into BCAA catabolism and exists as a mitochondrial (or in some reports peroxisomal) multienzyme complex composed of three units termed E1, E2, and E3. E1, which comprises two subunits (α and β), is involved in the decarboxylation of α-keto acids; E2 catalyzes the esterification of resulting aldehydes to HS-CoA; and E3 catalyzes their oxidation to acyl-CoAs (Mooney et al., 2002; Taylor et al., 2004). Although a role for BCKD in BCFA production has been suggested, direct evidence for its involvement in acyl sugar production has yet to be provided.

In both models, there is a requirement for branched-chain keto acid precursors provided by threonine deaminase (TD) and acetolactate synthase (ALS; Fig. 1). There is also a common requirement for BCKD in generating branched-chain acyl-CoAs from keto acids. The distinct elongation pathways and acyl sugar side chain compositions in these two species also imply the existence of different precursor pools and fluxes in the trichomes (Fig. 1). We have undertaken a genomic-based approach to further investigate, at the molecular level, acyl sugar biosynthesis in *S. pennellii* and *N. benthamiana*, in particular how BCFAs are produced and how their production is regulated. Our results indicate the role played by transcriptional regulation and support the existence of divergent pathway steps proposed in the two-pathway BCFA elongation model. The importance of key steps in BCFA production, such as BCKD and KAS, is indicated by functional analysis of gene knockdowns.

RESULTS

Acyl Sugar and Fatty Acid Production in *N. benthamiana* and *S. pennellii* Trichomes

To gain a better understanding of acyl sugar production in our model species, we first compared accumulation profiles of leaf exudates in *N. benthamiana* and *S. pennellii* (LA716). Acyl sugars collected from leaves were separated by HPLC, and their composition was analyzed by mass spectrometry. In parallel, the fatty acid composition of individual acyl sugars collected after HPLC was analyzed by gas chromatography. Stem exudates were also examined and were similar to leaf exudates in terms of yield and composition (data not shown).

One major and at least five minor acyl sugars were found in *N. benthamiana* trichome exudates (Supplemental Table S1). Exudates in methanol washes were composed predominantly of acyl sugars, and washes were shown to rapidly extract all acyl sugars (Supplemental Figs. S1 and S2). Their mass spectra were consistent with a Suc ester structure containing C_8 BCFAs (identified as 6MeC7:0 or 5MeC7:0 by gas chromatography-flame ionization detection [GC-FID]) and, as in other *Nicotiana* species, acetate (Ding et al., 2006; Supplemental Table S1). For instance, the major acyl sugar (molecular weight 636; Supplemental Table S1) consisted of one C_8 BCFA esterified to both the Glc and Fru subunits and one acetate esterified to the Fru subunit (Supplemental Fig. S3). Interestingly, esterification of aliphatic groups other than acetate to Fru has not been reported previously. The presence of acetic acid in the Fru unit of this major compound and some of the minor ones places these esters in the SE-III class, as described for *Nicotiana* species by Arrendale et al. (1990). A similar analysis confirmed that *S. pennellii* exudates contain a mix of Glc and Suc esters comprising branched short-chain fatty acids (2MeC3:0, 2MeC4:0, and 3MeC4:0) and branched or straight medium-chain fatty acids (8MeC9:0, C10:0, and C12:0; Supplemental Fig. S2C; Burke et al., 1987; Shapiro et al., 1994; Li et al., 1999).

Under our conditions, acyl sugar accumulation increased from younger to older leaves in *N. benthamiana*, and this was largely due to the major (molecular weight 636) form (Supplemental Fig. S4A). This equated to 10 μg cm^{-2} total fatty acids on the youngest leaves and about 30 μg cm^{-2} on the oldest leaves (Supplemental Fig. S4B), indicative of a relatively constant output from leaf to leaf. Under similar conditions, acyl sugar-associated fatty acid accumulation increased in *S. pennellii* from 150 μg cm^{-2} on the youngest leaves to 400 μg cm^{-2} on intermediate leaves and then decreased on subsequent leaves (Supplemental Fig. S4C). Overall, the leaf acyl sugar output was substantially higher in *S. pennellii* than in *N. benthamiana*. As in *N. benthamiana*, there were no major changes in the fatty acid composition of *S. pennellii* exudates on successive leaves (Supplemental Fig. S4C) or in the relative abundance of different acyl sugars (data not shown).

Analyses by scanning electron microscopy and light microscopy identified two main trichome types on *N. benthamiana* leaves. The first type, mostly present on the adaxial side (1–2 mm^{-2}; Fig. 2A), comprised a long stalk with a swollen base. The second and most abundant type consisted of smaller capitate trichomes with a thin stalk capped with one to four secretory cells (Fig. 2, A and C–E). These small trichomes secreted abundant viscous exudates, and their density ranged from 30 mm^{-2} in the youngest leaves to 5 mm^{-2} in older leaves (similar on both surfaces). In *S. pennellii*, there is one major trichome form classified as type IV or type d (Fig. 2B; Luckwill, 1943; Fobes et al., 1985). This has been shown to exude glucolipid-containing droplets (Fobes et al., 1985) that were later characterized in the same laboratory in more detail by Burke et al. (1987). Therefore, this trichome type appears largely responsible for acyl sugar secretion. This ranged in density from 50 mm^{-2} on young leaves to 10 mm^{-2} on mature leaves. Also present were a small number of type VI trichomes (2%−3% total; Fig. 2F; Luckwill, 1943). The higher level of acyl sugar output in *S. pennellii*, despite comparable trichome density between the two species, suggests that the type IV trichome could be the more productive.

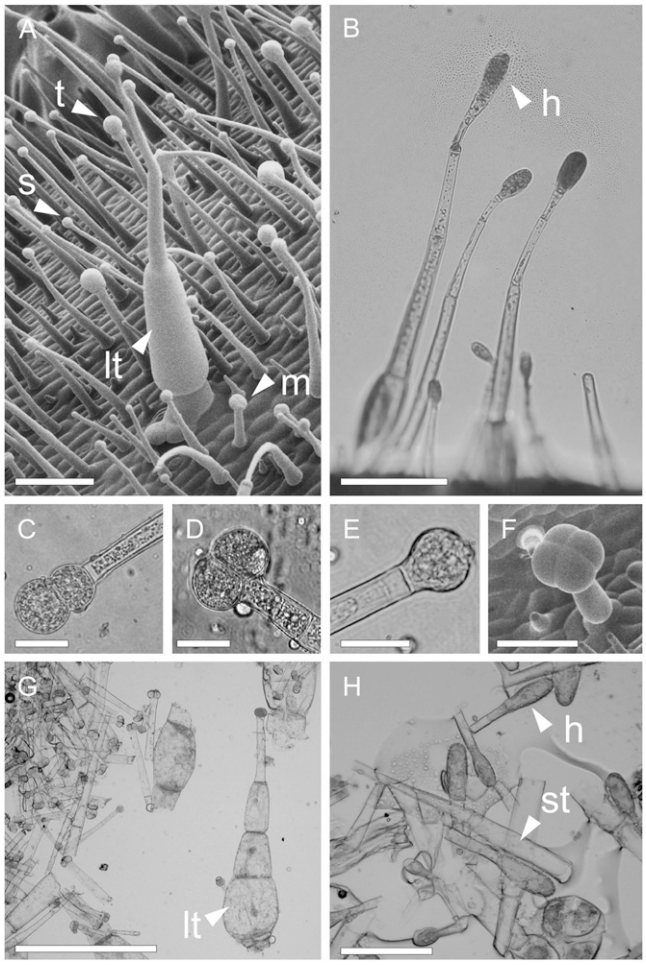

Figure 2. Glandular trichomes in *N. benthamiana* and *S. pennellii*. A, Scanning electron microscopy of a *N. benthamiana* stem shows one large swollen-stalk trichome (lt) and small trichomes capped with single (s), twin (t), or multiple-celled (m) secretory heads. Bar = 200 μm. B, Light microscopy of acyl sugar-secreting type IV trichomes of *S. pennellii*, indicating a glandular head (h). Bar = 200 μm. C to E, Common glandular head types of small secretory trichomes in *N. benthamiana*. Bars = 20 μm. F, *S. pennellii* type VI glandular trichome visualized with scanning electron microscopy. Bar = 100 μm. G, Trichomes harvested from leaves of *N. benthamiana* by brushing, including large type (lt). Bar = 500 μm. H, Trichomes similarly harvested from *S. pennellii* leaves showing glandular heads (h) and broken stalks of type IV trichomes (st). Bar = 100 μm.

Microarray Analysis of Gene Expression in Trichomes of *S. pennellii* and *N. benthamiana*

To identify genes (or gene families) involved in the acyl sugar production pathway and gain insight into the role of transcriptional regulation in glandular trichomes, we used TOM2 Affymetrix oligonucleotide arrays representing about 12,000 tomato genes and profiled transcripts that preferentially accumulate in the trichomes of *N. benthamiana* and *S. pennellii*. RNA for the microarray was obtained from leaf trichomes and leaves from which trichomes had been removed, and gene expression was compared between the two samples. Trichome-harvesting methodology was effective at removing stalked glandular trichome types from leaves with minimal contamination of trichome harvests by nontrichome cells (Fig. 2, G and H). Consequently, harvests contained abundant small capitate trichomes and a few large swollen-base glandular trichomes from *N. benthamiana* and, in the case of *S. pennellii*, both the majority type IV trichomes and very low levels of the minority type VI glandular heads. The presence of more than one trichome type might lead to underestimation of trichome-leaf gene expression ratios for some metabolic pathways, but trichomes responsible for producing acyl sugars appeared to be the most abundant. Despite the divergence in sequence between *N. benthamiana* and tomato

genes, we found that a similar proportion of the genes in *N. benthamiana* (81%) and *S. pennellii* (75%) produced a significant signal on the microarrays. This result was consistent with previous observations (Rensink et al., 2005). It was considered likely, however, that further verification of microarray data by real-time reverse transcription (RT)-PCR of specific isogenes would be required due to the possibility of cross-hybridization within gene families.

Comparison of the microarray data from the two species highlighted many overall similarities in gene expression in trichomes, despite strong differences in trichome morphology (Figs. 2 and 3; Supplemental Tables S2 and S3). The number of genes preferentially expressed in total trichomes in relation to total underlying leaf tissues was comparable (111 and 156 in *N. benthamiana* and *S. pennellii*, respectively, at a leaf trichome-total underlying leaf expression ratio > 2), and the overlap was high (20% of preferentially trichome-expressed genes and 35% of those reduced in expression were common to both species; Supplemental Table S4). Consistent with low chlorophyll levels measured in trichome harvests (10% of underlying leaf levels by dry weight; Supplemental Table S5), the photosynthetic genes were widely repressed (Fig. 3). Conversely, many trichome-enriched mRNAs were associated with nonphotosynthetic metabolism (36% in both species), cell signaling, and transcription. This suggested that trichomes in both species were metabolically very active and probably dependent to an extent on other leaf tissues for photosynthate (Fig. 3). Genes responsible for lipid metabolism were highly expressed in both trichomes, and those encoding lipid transfer proteins, which have a putative role in epicuticular wax transport, were especially well represented in *N. benthamiana* trichomes (Table I). Abundance of lipid transfer protein gene expression has also been noted in alfalfa (*Medicago sativa*), mint (*Mentha piper-*

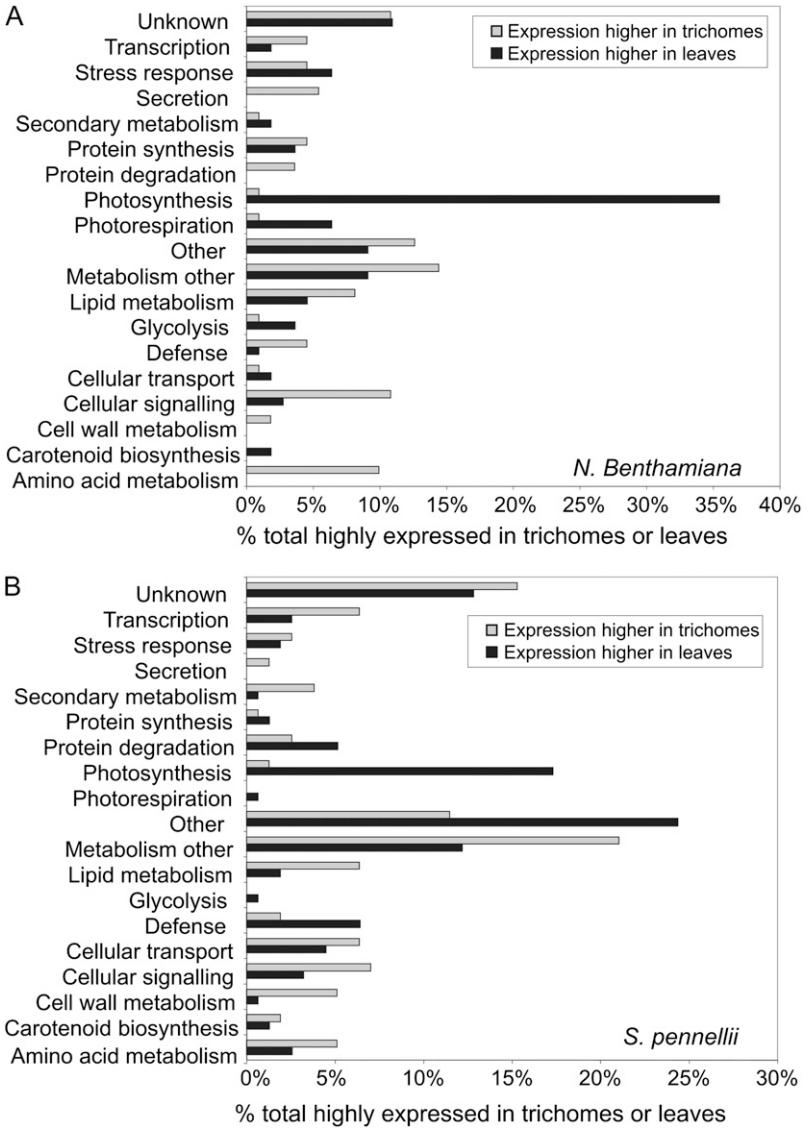

Figure 3. Functional classification of differentially expressed genes in the trichomes of *N. benthamiana* and *S. pennellii*. Functional assignment is shown for the products of genes that are preferentially expressed in leaf trichomes or total underlying leaf in *N. benthamiana* (A) and *S. pennellii* (B). These genes showed at least a 2-fold difference in expression. The *y* axis lists categories of putative gene function, and the *x* axis shows the proportion of preferentially trichome-expressed genes in a given functional category.

Table I. *Genes associated with amino acid metabolism and secretory processes that are preferentially expressed in N. benthamiana or S. pennellii leaf trichomes*

The genes that are represented have a putative function in metabolism or secretion, according to their annotation. Expression ratios refer to the level of expression of any given gene in trichomes compared with its expression in underlying leaf tissues. Annotations correspond to the description of the protein that is most closely related to the predicted product of each gene. Genes associated with BCAA biosynthesis are shown in boldface.

Unigene Number	Expression Ratio	Annotation
N. benthamiana		
Amino acid metabolism		
SGN-U232722	**10.1**	**2-Isopropylmalate synthase [*S. pennellii*]**
SGN-U212594	8.0	His decarboxylase [*Solanum esculentum*]
SGN-U212595	7.4	His decarboxylase [*S. esculentum*]
SGN-U221864	**7.0**	**Putative dihydrolipolyacyltransferase subunit of the BCKD complex [*Oryza sativa*]**
SGN-U217800	**6.2**	**Putative 3-isopropylmalate dehydratase large subunit [*O. sativa*]**
SGN-U216021	**5.1**	**3-Isopropylmalate dehydrogenase [*Brassica napus*]**
SGN-U218657	2.7	Pyridoxamine-phosphate oxidase [Arabidopsis]
SGN-U216620	2.6	Asp aminotransferase, cytoplasmic (transaminase A)
SGN-U215900	**2.4**	**Putative Thr dehydratase/deaminase [*O. sativa*]**
SGN-U221078	2.1	Orn decarboxylase [*S. esculentum*]
SGN-U221033	**2.1**	**Isovaleryl-CoA dehydrogenase [*S. tuberosum*]**
Putative secretion		
SGN-U231540	6.6	Pleiotropic drug resistance-like protein [*N. tabacum*]
SGN-U222218	6.6	Nonspecific lipid transfer protein [*S. esculentum*]
SGN-U232089	2.8	TSW12 (putative lipid transfer protein) [*S. esculentum*]
SGN-U216923	2.7	Putative lipid transfer protein, glycosylphosphatidylinositol-anchored [*Cicer arietinum*]
SGN-U212736	2.6	Nonspecific lipid transfer protein [*S. esculentum*]
SGN-U232089	2.2	LETSW12 *S. esculentum* TSW12 mRNA (putative lipid transfer protein)
S. pennellii		
Amino acid metabolism		
SGN-U221864	**6.5**	**Putative dihydrolipolyacyltransferase subunit of the BCKD complex [*O. sativa*]**
SGN-U226908	4.9	Putative dihydrodipicolinate reductase-like protein [*O. sativa*]
SGN-U213768	**3.9**	**Acetolactate synthase SuRB**
SGN-U215900	**3.5**	**Putative Thr dehydratase/deaminase [*O. sativa*]**
SGN-U213163	3.3	CIG1 (Pro oxidase) [*N. tabacum*]
SGN-U213162	3.3	Pro oxidase/dehydrogenase 2 [*N. tabacum*]
SGN-U214608	**3.0**	**DIN4 (DARK-INDUCIBLE4); 3-methyl-2-oxobutanoate dehydrogenase [Arabidopsis]**
SGN-U215085	2.9	Gln synthetase (Glu-ammonia ligase)
Putative secretion		
SGN-U222218	2.7	Nonspecific lipid transfer protein [*S. esculentum*]
SGN-U212736	2.5	Nonspecific lipid transfer protein [*S. esculentum*]

ita), and basil (*Ocimum basilicum*) trichomes (Lange et al., 2000; Gang et al., 2001; Aziz et al., 2005).

Despite these similarities between tobacco and tomato trichomes, there were notable exceptions. For instance, defense-related genes were only up-regulated in *N. benthamiana* trichomes; conversely, secondary metabolism genes were only elevated in *S. pennellii* trichomes (Fig. 3). In the latter case, genes for flavonoid metabolism were highly represented, which concurs with the presence of flavonoids in the exudates of this species along with acyl sugars (Supplemental Table S3; Fobes et al., 1985).

Genes involved in amino acid metabolism were highly expressed in trichomes of both species (Fig. 3), and interestingly, those with potential involvement in acyl sugar synthesis were prominent (Table I). Components of the BCKD complex, E2 (dihydrolipoyl acyltransferase) and E1-β (DIN4) subunits, involved in branched-chain catabolism, were represented in both species. Significantly, genes responsible for the three α-KAE steps (*IPMS*, *IPMD*, and *IPDS*) were strongly expressed only in *N. benthamiana* trichomes. Conversely, those required for the branched-chain keto acid precursors ALS and TD were possibly more highly expressed in *S. pennellii*.

In conclusion, common patterns of gene expression were observed in the trichomes from *N. benthamiana* and *S. pennellii* that were consistent with their primary role as glandular secretory structures. Differences were also noted that pointed toward evolutionary divergence in secondary metabolism, in particular divergent acyl sugar elongation mechanisms and the role of the trichome as a defensive structure. This analysis, therefore, provided a platform for a molecular understanding of trichome metabolism.

Real-Time RT-PCR Analysis of Specific Genes of the BCAA Synthesis Pathway and the BCKD Complex

Given the high level of transcriptional regulation suggested by the microarray analyses in trichome BCAA synthesis and breakdown, real-time RT-PCR

analysis was carried out to test these findings and address possible cross-hybridization issues (Table II). Gene-specific real-time RT-PCR primers were designed against database tobacco and tomato sequences showing 100% homology to the microarray probe (Supplemental Tables S6 and S7). In the cases of *IPMS A* and *B* and *BCKD* E1-β, sequence data from *N. benthamiana* was obtained for this purpose by RT-PCR (Supplemental Table S6).

Importantly, high preferential trichome expression was consistently observed in both plants for the genes encoding E2 and E1-β components of the BCKD complex (Table II). This underlined the importance of this enzyme in the trichomes of both species. In the case of the α-KAE pathway, which is proposed to play a key role in *N. benthamiana*, we confirmed that the first committed step carried out by *IPMS* is strongly elevated in the trichomes in this species (Table II). Real-time RT-PCR analysis suggested that a particular isogene, *IPMS C* (ESTs are described in Supplemental Table S7), was induced rather than the tobacco homolog of tomato *IPMS B*, as indicated by the microarray. The discrepancy could have arisen from cross-hybridization of the *IPMS B* probe with *IPMS C* transcript, which was not represented in the array. The real-time analysis indicated that isoforms IPMS A and B (which are closely related to the Arabidopsis gene candidates for Leu synthesis; Supplemental Table S7; de Kraker et al., 2007) are actually repressed in *N. benthamiana* trichomes and not strongly elevated in *S. pennellii*. In the case of *IPMD*, the second step in α-KAE, we confirmed that this gene is highly expressed in *N. benthamiana* trichomes (Table II). For the final step, the increase in *IPDS-L* in tobacco trichomes seen by microarray remained unconfirmed by RT-PCR but might be due to isogenes not yet represented in the EST database (only one contig was available but four isogenes were present in Arabidopsis; Supplemental Table S7). Some increases were seen in *IPMD* and *IPDS-L* in wild tomato trichomes, however, confirming slight increases seen in the microarray. Interestingly, elevated trichome-total underlying leaf expression ratios for ALS and TD observed in *S. pennellii* trichomes by microarray were confirmed by real-time RT-PCR. This supported the notion of high flux into the BCAA pathway in trichomes in this plant.

Therefore, overall, it was confirmed by real-time RT-PCR analysis that the BCKD complex, long proposed to undertake the catabolic step required for the BCFA synthesis pathway, is up-regulated in trichomes of both species. A key difference between the species was noted in that the specific role proposed for the α-KAE pathway in *N. benthamiana* was supported by elevation of the first two steps of the pathway in trichomes of this species. In the case of *S. pennellii*, the importance of ALS and TD in providing keto acid precursors (2-keto-3-methyl valerate and 2-ketoisovalerate; Fig. 1A) was also suggested. Overall, these observa-

Table II. *Trichome/leaf gene expression ratios determined by microarray analysis and real-time RT-PCR*

Gene Product	Alias	*N. benthamiana*						*S. pennellii*					
		Microarray		Real-Time RT-PCR[a]				Microarray		Real-Time RT-PCR			
				Set 1		Set 2				Set 1		Set 2	
		Ratio	*P*	Ratio	SD	Ratio	SD	Ratio	*P*	Ratio	SD	Ratio	SD
BCAA synthesis													
Acetolactate synthase	SuRA[b]	NC[c]	–	–	–	–	–	3.9[d]	0.09	9.0	2.0	28.4	5.1
Thr dehydratase/deaminase	TD	2.4	0.05	–	–	–	–	3.5	0.09	3.9	1.0	16.9	3.2
2-Isopropylmalate synthase	IPMS A	NC	–	0.2	0.04	0.4	0.1	1.9	0.09	1.4	0.4	2.8	0.8
	IPMS B	10.1	0.02	0.4	0.04	0.6	0.1	NC	–	1.7	0.4	1.0	0.2
	IPMS C	–	–	14.8	3.4	27.4	2.0	–	–	–	–	–	–
3-Isopropylmalate dehydrogenase	IPMD	5.1	0.04	3.4	0.3	5.5	0.4	1.7	0.10	4.2	0.9	11.5	2.1
3-Isopropylmalate dehydratase (large subunit)	IPDS-L	6.2	0.03	0.4	0.1	0.6	0.0	1.9	0.09	2.4	0.6	5.9	1.2
BCAA degradation													
Branched-chain α-keto acid dehydration													
E1-β subunit	β-BCKD	NC	–	14.1	3.0	4.6	0.5	3.0[d]	0.09	4.1	0.9	9.8	1.9
E2 subunit	BCKD E2	7.0	0.03	4.6	0.7	13.0	1.3	6.5[d]	0.09	11.8	3.2	48.2	15.3
Fatty acid elongation													
β-Ketoacyl-ACP synthase IIIA	KAS IIIA	NC	–	–	–	–	–	1.5	0.09	2.8	0.6	4.2	0.8
β-Ketoacyl-ACP synthase I	KAS IA	–	–	–	–	–	–	–	–	2.3	0.7	2.3	0.4
	KAS IB	–	–	–	–	–	–	–	–	5.4	1.3	19.1	3.9
	KAS IC	–	–	–	–	–	–	–	–	9.7	4.2	2.8	1.8
Control													
Glyceraldehyde 3-phosphate dehydrogenase	GAPDH	–	–	0.9	0.2	0.6	0.1	–	–	1.4	0.4	1.1	0.3

[a]Real-time RT-PCR data sets 1 and 2 were obtained from plants grown on two separate occasions, using actin normalization. [b]TOM2 probe annotated as SuRB (Table I) matches current SGN entry annotated as SuRA (Supplemental Table S7). [c]NC, No significant change observed. [d]Data verified with more than one real-time RT-PCR primer pair (Supplemental Table S6).

tions were consistent with the expected importance of these pathways in providing precursors for acyl sugar production, but important differences in elongation step mechanisms were also highlighted.

BCKD Plays a Critical Role in BCFA and Acyl Sugar Production

To determine the significance of the trichome gene expression data, we undertook a comprehensive analysis of the role played by selected components of the BCKD complex in BCFA and acyl sugar production using virus-induced gene silencing (VIGS).

In primary metabolism, the first committed step in BCAA degradation is catalyzed by the BCKD complex (Mooney et al., 2002). As we had found genes encoding the E2 and E1-β components to be expressed at particularly high levels in trichomes (Table II), we also examined the expression of genes encoding other components of BCKD. We identified three tomato unigenes encoding α-subunits of the E1 component (α-BCKD I to III; Supplemental Table S7). We found from transcript measurement by RT-PCR that the genes encoding α-BCKD I, α-BCKD II, and β-BCKD, but not α-BCKD III, were expressed at very high levels in leaf and stem trichomes (Fig. 4A).

To test the importance of BCKD in acyl sugar production, we targeted for silencing the gene encoding the β-subunit of E1 using VIGS and tobacco rattle virus-based vectors (Liu et al., 2002a). The down-regulation of E1-β in *N. benthamiana* led to a significant reduction in acyl sugar accumulation. The five main acyl sugar peaks, identified by liquid chromatography-mass spectrometry (LC-MS), were all reduced in the BCKD knockdown by 2- to 5-fold relative to controls (Fig. 4B). A 3-fold reduction in total acyl sugar fatty acids was also observed, without change in fatty acid composition (Fig. 4C). This decrease correlated with an 8-fold reduction of E1-β transcript levels, as determined by real-time RT-PCR (Table III). The silenced plants were morphologically similar to controls, and trichome densities were unaffected (data not shown), which argued against the reduction in acyl sugar chain production being the indirect consequence of a growth defect. To address further the issue of direct cause and effect, wax composition was examined in *N. benthamiana* and found to consist predominantly of an equal mix of straight odd-number alkanes and branched *iso* or *anteiso* chains. In the BCKD knockdown, total alkane levels were unchanged but the *iso*- and *anteiso*-alkanes were reduced considerably, with a compensatory increase in straight chains (Fig. 4D). This suggests that there was a specific impact on branched-chain products (both acyl sugar side chains and branched alkanes) requiring BCKD rather than an indirect metabolic or secretory defect leading to reduced acyl sugar output.

The use of VIGS for down-regulating genes of the cultivated tomato (*Solanum lycopersicum*) has been documented (Liu et al., 2002a). To test whether this method is also effective in the wild relative *S. pennellii*, we first used it to target the phytoene desaturase (PDS) gene for silencing. TRV2-PDS-treated plants displayed extensive photobleaching, which is symptomatic of PDS down-regulation (Fig. 5D). On the basis of this result, we applied VIGS to assess the role of BCKD in acyl sugar production in this species. Silencing the gene encoding the β-subunit of E1 (E1-β) produced a significant reduction in 8MeC9:0 (by 40%) and 2MeC3:0. In contrast, the SCFAs C10:0 and C12:0, which are not derived from BCAAs, showed a compensatory increase of 40% (Fig. 4E). As in *N. benthamiana*, these metabolic changes occurred in the absence of any deleterious effect on growth or trichome density (data not shown). Wax alkane components were also examined in *S. pennellii* leaves and found to constitute a significant branched-chain component. In the knockdowns, a significant 30% reduction of the major branched-chain component, *iso*-C_{31} alkane, was observed (Fig. 4F). Overall, these data suggested that the BCKD knockdown was specifically affecting branched-chain production in both species.

The less dramatic but significant metabolic effects of E1-β silencing seen in *S. pennellii*, in comparison with *N. benthamiana*, may have been caused by lower efficiency of VIGS in the wild tomato species, although in this experiment we still detected a 3- to 4-fold reduction in transcript levels in both leaves and leaf trichomes (Table III). Nevertheless, our results clearly indicated that BCKD plays a critical role in BCFA production in both species. In *S. pennellii*, the observed rise in SCFA content appears to compensate for the reduction in BCFA. As a possible consequence of this compensation, total acyl sugar amount was not affected by E1-β silencing in the wild tomato species (data not shown). A similar compensatory effect was particularly clear with *N. benthamiana* waxes, in which there is also a mix of branched and straight chains in the alkane component.

Branched-Chain Acyl-CoAs Accumulate in *S. pennellii* Trichomes

BCKD converts branched-chain keto acids to branched-chain acyl-CoAs with the loss of one carbon. According to the proposed elongation models, short branched-chain acyl-CoAs, MeC3:0, 2MeC4:0, and 3MeC4:0 in *S. pennellii* and 5MeC7:0 and 6MeC7:0 in *N. benthamiana*, are the principal products of BCKD (Fig. 1). We compared the acyl-CoA composition of trichome extracts with that of extracts from stems or leaves from which trichomes had been removed. Significant levels of MeC3:0, 8MeC9:0, and C10:0-CoAs were seen in *S. pennellii* stem and leaf trichomes, compounds that could not be found in underlying tissues (Fig. 5, A and B). These three branched-chain CoA species corresponded to the major acyl chain components of *S. pennellii* acyl sugars. MeC3:0-CoA is an expected product of BCKD that also would be required for priming elongation by FAS to generate 8MeC9:0. The presence of 8MeC9:0 and C10:0-CoAs in

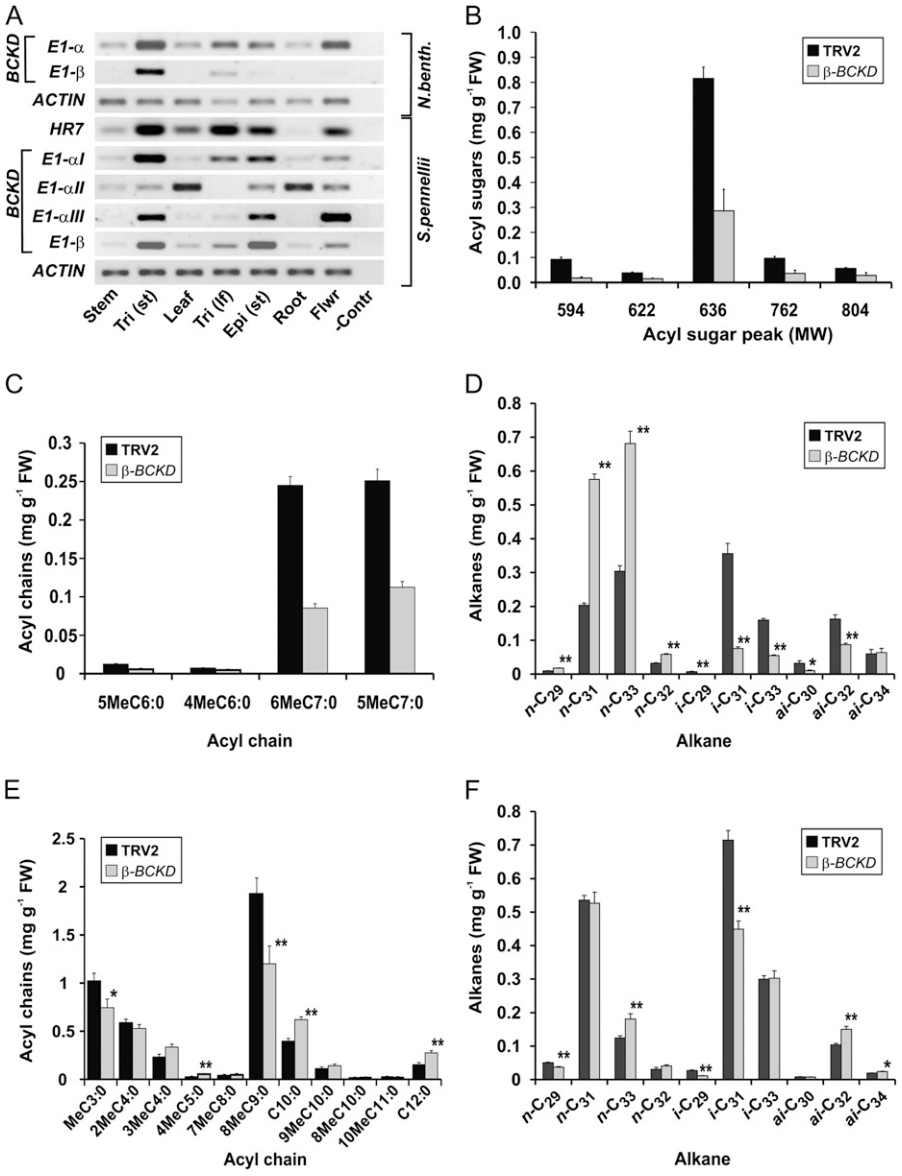

Figure 4. Acyl sugar and wax alkane production of *N. benthamiana* and *S. pennellii* plants impaired in BCAA breakdown. Analysis of BCKD gene expression (A) and function by gene knockdown using VIGS (B–F). A, Semiquantitative RT-PCR analysis of the expression of genes encoding components of the BCKD complex in different tissues of *N. benthamiana* and *S. pennellii*. Tri (st), Stem trichomes; Tri (lf), leaf trichomes; Epi (st), stem epidermis; Flwr, flower; −Contr, no cDNA PCR control. cDNA levels were normalized according to actin transcript levels. The gene encoding HR7, highly expressed in trichomes and epidermis of tomato and tobacco, served as an additional control. B, Major acyl sugars in young *N. benthamiana* leaf exudates after *BCKD* E1-β silencing, separating methanol extracts by LC-MS. Control plants were treated with a TRV2 vector containing no insert. Acyl sugars are defined by their molecular mass (Supplemental Table S1) and their approximate abundance measured by comparison with the internal standard Suc monolaurate. Error bars indicate SE ($n = 8$). Significant differences are as follows: $P < 0.01$ (molecular weight 594–762), $P < 0.05$ (molecular weight 804). FW, Fresh weight. C, Composition of FAMES derived from *N. benthamiana* total acyl sugars separated in B. Error bars indicate SE ($n = 8$; $P < 0.01$). D, Wax alkane composition of a young *N. benthamiana* leaf after *BCKD* E1-β silencing, separated by gas chromatography-mass spectrometry. Error bars indicate SE ($n = 4$). *n*-C_{29}, Nonacosane; *n*-C_{31}, hentriacontane; *n*-C_{33}, tritriacontane; *n*-C_{32}, dotriacontane; *i*-C_{29}, 2-methyloctacosane; *i*-C_{31}, 2-methyltriacontane; *i*-C_{33}, 2-methyldotriacontane; *ai*-C_{30}, 3-methylnonacosane; *ai*-C_{32}, 3-methylhentriacontane; *ai*-C_{34}, 3-methyltritriacontane. E, Composition of FAMES derived from *S. pennellii* acyl sugars extracted in methanol from young expanded leaves. Error bars indicate SE ($n = 12$). F, Wax alkane composition in *S. pennellii*. Error bars indicate SE ($n = 6$). In D to F, asterisks denote significant differences (* $P < 0.05$, ** $P < 0.01$) obtained using Student's *t* test.

Table III. *Quantification of silencing in VIGS experiments by real-time RT-PCR*

Plant	Gene Target	Leaf		Trichome	
		Expression Ratio[a]	SE	Expression Ratio[a]	SE
N. benthamiana	*BCKD* E1-β	0.12	0.03	–	–
S. pennellii	*BCKD* E1-β	0.37	0.12	0.24	0.04
	KAS IA	0.14	0.02	0.30	0.03
	KAS IB	0.66	0.09	0.63	0.05

[a]Expression level in silenced tissue relative to the TRV2 control ($n = 3$).

trichomes is consistent with export occurring from the plastid of the corresponding BCFAs. Branched-chain acyl-CoAs were not detected in *N. benthamiana* (data not shown). This could be due to the lesser acyl sugar output of *N. benthamiana* or might relate to the differing elongation pathways or compartmentation proposed for the two species (Fig. 1).

Taken together with the high trichome gene expression levels for BCAA metabolism and functional data for BCKD (indicating its requirement for acyl sugar synthesis), the accumulation of trichome branched-chain acyl-CoAs is consistent with the operation of BCKD and the synthesis of BCFAs in *S. pennellii* trichomes. Similar evidence was not found for *N. benthamiana* but could be sought in tobacco species with higher outputs.

Role of FAS and Differential Roles of *KAS I* Genes in BCFA Elongation in *S. pennellii*

Labeling studies suggested that BCFA destined for acyl sugars are formed by two-carbon elongation steps in *S. pennellii* but not in *N. benthamiana* (van der Hoeven and Steffens, 2000; Kroumova and Wagner, 2003). Genes associated with lipid metabolism were elevated in trichomes in the microarray analysis, although few were directly related to plastidial FAS, which was unexpected, especially for *S. pennellii*. The requirement of FAS, therefore, was tested in this plant by measuring the effects of cerulenin on acyl sugar production in leaves. Plastid-localized KAS I and KAS II enzymes are sensitive to this inhibitor, whereas cytosolic elongation is not (Koo et al., 2005). Mitochondrial KAS from Arabidopsis is also sensitive to this inhibitor (Yasuno et al., 2004). In this experiment, de novo production was monitored in isolated leaves of *S. pennellii* that had been stripped of their acyl sugars and placed for 5 d in cerulenin or control solutions. It was previously determined that ethanol-washed leaves start producing acyl sugars after 1 to 2 d and build up a secreted layer for up to 5 d (Supplemental Fig. S5). Cerulenin treatments resulted in a significant decrease (50%) of both BCFAs and SCFAs in acyl sugars but only those of C_{10} and above (Fig. 5C). These results suggested that the activities of KAS I and/or KAS II enzymes are involved for both the branched and straight medium-chain fatty acid elongation in the trichome exudates.

To support these findings and to assess which specific enzymes may be involved in BCFA elongation, we proceeded to silence specific KAS genes that were well represented in tomato EST databases. Our analysis of existing ESTs identified three possible KAS I enzymes (medium-chain length specificity) and four putative KAS II enzymes (long-chain length specificity) in tomato (Supplemental Table S7). This multiplicity of enzymes may be a consequence of ploidization events or could point toward specialization, as Arabidopsis expresses only one KAS gene for each of these two classes (Beisson et al., 2003). The expression profiles of the seven genes were first determined in all tissues by semiquantitative RT-PCR (Supplemental Fig. S6). This analysis suggested increased expression in leaf and stem trichomes, relative to underlying tissues, for KAS IB and KAS IIC. Real-time RT-PCR measurement of the three KAS I gene transcripts indicated that KAS IB followed by KAS IC showed the highest trichome expression, with only a 2-fold increase for KAS IA, in relation to underlying leaf tissue (Table II).

To determine whether the expression pattern of these genes is related to a specific role in trichome metabolism (and on the basis of expected chain length substrate specificity of KAS I enzymes), we targeted *KAS IA* to *IC* for down-regulation by VIGS (Table III). Silencing *KAS IA* and *KAS IB* produced the clearest metabolic phenotype, resulting in a reduction in branched-chain synthesis. This occurred without change in growth, development, or trichome density, although *KAS IA*-silenced plants showed limited signs of chlorosis (possibly due to the requirement of KAS IA for FAS in leaves; Fig. 5D). Wild-type plants were previously observed to synthesize the C_{10} fatty acids at a branched-chain to straight-chain ratio of approximately 2 consistently throughout the plant (Supplemental Fig. S4C). In the silencing experiments, knockdown of *KAS IA* or *KAS IB* reduced the ratio to less than 1 (compared with TRV2 empty vector controls, for which the ratio was 2). This amounted to a significant 30% reduction of the major BCFA 8MeC9:0 and doubling of C10:0 (Fig. 5E). The fatty acid profile of acyl sugars in these plants suggested that flux through the elongation of BCFAs and SCFAs had decreased and increased, respectively. This model was supported by the trichome acyl-CoA profiles of plants silenced in *KAS IA* and *IB*. In both cases, straight-chain acyl-CoAs (C_{10} and C_{12}) accumulated to similar or higher levels in relation to branched-chain acyl-CoAs (8MeC9:0, 9MeC10:0, and 10MeC11:0),

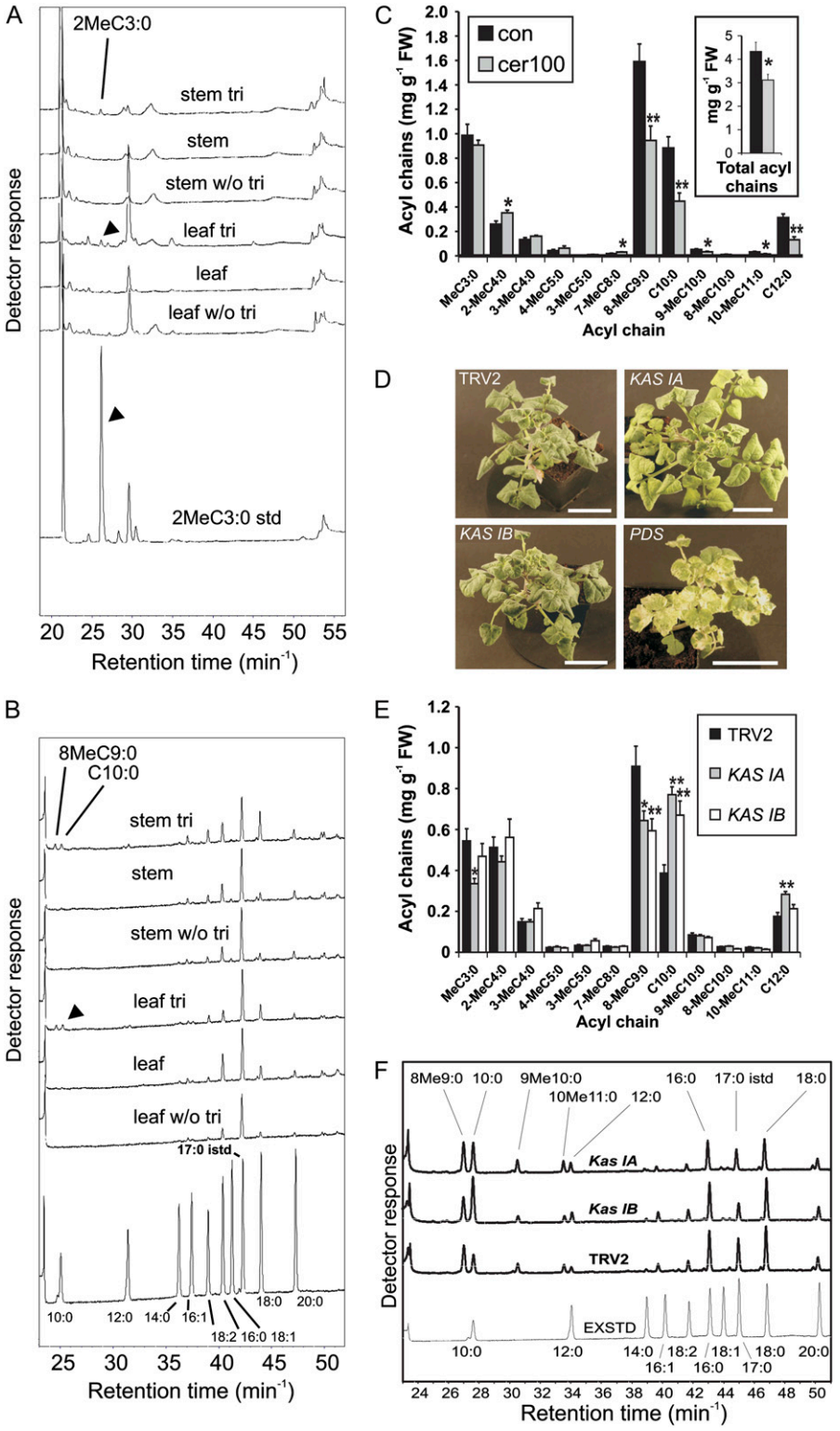

Figure 5. Role of fatty acid synthesis in acyl sugar side chain production in *S. pennellii* trichomes. Acyl-CoAs were measured in wild-type trichomes (A and B), and the effects of cerulenin inhibition (C) and *KAS I* gene silencing (D–F) were determined. A and B, Acyl-CoA profiles of *S. pennellii* leaf and stem trichome extracts compared with extracts from total underlying leaf and stem tissues. Acyl-CoA chains below C10:0 were separated with a porous graphite carbon column (A). C10:0 and over were separated with a C18 column (B). Internal standard was 0.2 pmol mg^{-1} fresh weight (FW) heptadecanoyl-CoA (17:0). tri, Trichome. C, Effect of cerulenin on acyl sugar fatty acid composition; values represent the abundance of FAMES derived from leaf acyl sugars extracted with methanol. The inset shows the sum of acyl sugar-derived FAMES. con, Controls; cer 100, 100 μM cerulenin. Error bars indicate SE ($n = 10$). Asterisks denote significant differences (* $P < 0.05$, ** $P < 0.01$) using Student's *t* test. D, Morphology of a *S. pennellii* plant in which *KAS IA* and *KAS IB* were down-regulated using VIGS, compared with plants treated with a TRV2 control strain or in which the *PDS* gene was silenced. Bars = 8 cm. E, Composition of acyl sugar-derived FAMES from young expanded leaves in which *KAS I* genes were down-regulated using VIGS. Control plants were treated with a TRV2 vector containing no insert. Error bars indicate SE ($n = 8$). Significant differences relative to the TRV2 control are as follows: * $P < 0.05$, ** $P < 0.01$. F, Acyl-CoA HPLC profiles of trichomes in plants in which *KAS IA* or *KAS IB* was down-regulated using VIGS. EXSTD, Mixture of different fatty acid standards; the internal standard used in this experiment was C17:0 at 0.2 pmol mg^{-1} fresh weight of plant material.

whereas control plants displayed less straight-chain than branched-chain acyl-CoAs. There was notably less effect on long-chain acyl-CoAs (C_{16}–C_{18}), which, taken together with the low impact of the knockouts on plant morphology, suggests that there may be redundancy at the level of membrane lipid synthesis in trichomes (Fig. 5F). There was also no impact on the composition and amounts of leaf C_{16} to C_{18} fatty acids

(data not shown). In contrast, and despite its relatively high levels of expression in leaf trichomes, silencing *KAS IC* caused little change in acyl sugar (or membrane lipid fatty acid) composition, and these plants also appeared phenotypically normal (data not shown). Taken together, these data support the role of plastidial FAS in BCFA synthesis in *S. pennellii* and implicate specific KAS I isoforms in their production. They also suggest that branched-chain and straight-chain FAS pathways compete for precursors and that KAS I enzymes have different levels of involvement in FAS in the trichome and elsewhere in the plant.

DISCUSSION

In this study, we have used a comparative genomic approach to investigate the biosynthesis of trichome acyl sugars in the Solanaceae. Our analysis involved two species, *N. benthamiana* and *S. pennellii*, which have contrasting acyl sugar accumulation profiles and divergent proposed pathways leading to the production of their BCFA components. Using microarray and real-time RT-PCR analyses, we showed that, in both species, the expression of genes involved in the production and breakdown of BCAAs is higher in trichomes than in underlying leaf tissue. Importantly, genes responsible for α-KAE were among the most up-regulated in trichomes of *N. benthamiana*, supporting the operation of this pathway in tobacco species. Interestingly, genes required for branched-chain keto acid precursor provision, ALS and TD, were highly expressed in *S. pennellii*. The relatively low expression in trichomes of genes associated with photosynthesis suggests that the trichomes are relying to a significant degree on imported carbon for acyl sugar production.

The results of our functional analysis show that the enzyme complex BCKD, which catalyzes the decarboxylation of keto acids to generate acyl-CoAs, is implicated in the biosynthesis of BCFAs destined for acyl sugars and for branched wax alkanes in both species. In addition, the results of inhibitor treatment and VIGS data indicate that the FAS complex and in particular two isoforms of KAS I play an important role in BCFA elongation for acyl sugar synthesis in *S. pennellii*. These results highlight some of the molecular mechanisms that underlie the diversity of trichome metabolism in the Solanaceae.

Importance of BCAA Production and Breakdown Pathways in Acyl Sugar-Producing Trichomes

We showed that the production of acyl sugars in trichomes is associated with the elevated expression of genes encoding enzymes of both BCAA biosynthesis and BCAA breakdown pathways. Branched-chain acyl-CoAs produced from keto acids (by BCKD) are proposed to channel into acyl sugar production rather than undergo complete degradation (Kandra et al., 1990). Given that detached trichomes have been shown to be capable of synthesizing acyl sugars in *N. benthamiana* and other tobacco species, our finding that up-regulation of BCAA metabolism genes occurs in these cells in both model species is consistent with acyl sugar synthesis occurring there (Kandra and Wagner, 1988; Kroumova and Wagner, 2003). Taken together with the measurable accumulation of branched-chain acyl-CoAs in *S. pennellii* trichomes, these findings signal the importance of these pathways in providing precursors for BCFA production. Our analysis does not exclude other leaf cell types from synthesis capability but points toward the importance of trichomes.

Of the genes encoding BCAA breakdown enzymes, those encoding components of the BCKD complex were strongly induced in trichomes of both species. Our functional analysis suggests that the BCKD complex plays a central role in acyl sugar formation in both *S. pennellii* and *N. benthamiana*. Silencing of the β-subunit of the E1 component of BCKD by VIGS reduced acyl sugar levels by 3-fold in *N. benthamiana* and reduced the levels of BCFAs by approximately 40% in *S. pennellii*. Branched-chain wax alkanes were also reduced in both species. Therefore, BCKD would appear to be essential for the operation of α-KAE (in tobacco acyl sugar synthesis) and in precursor supply for BCFA elongation by FAS (for tomato acyl sugar production and for wax synthesis in both species).

While the importance of the complex is clear, the question remains of its substrate specificity and of how its proposed substrates and products transit between cell compartments, given the reported location of this complex in plants to the mitochondrion (or possibly the peroxisome; Taylor et al., 2004). In *N. benthamiana*, C_9 branched-chain keto acids are the expected substrates, and these might be generated in the plastid, which is the site of the α-KAE enzymes responsible for Leu synthesis (Fig. 1; Binder et al., 2007). According to this scenario, intracellular transport of substrate would be required either as keto acid or as extended BCAAs. Intracellular targeting of the key enzymes must also be established in trichomes, however. Direct evidence for the existence of novel extended BCAAs in Solanaceae trichomes has not yet been provided. Nevertheless, it is noteworthy that extended Leu-based amino acids have been detected in leaves of Arabidopsis overexpressing *MAM1*, one of the *IPMS* genes for glucosinolate production, without any apparent detrimental effect on the plant (Field et al., 2006). How and where the acyl-CoAs produced by the BCKD complex become substrates for acyl sugar formation in *N. benthamiana* also remain to be established. In *S. pennellii*, glucosyl transferases utilizing fatty acids (not acyl-CoAs) appear to be responsible for the first step incorporating acyl chains onto acyl sugars. The intracellular location of these enzymes is not known, although the subsequent disproportionation step could occur at the endoplasmic reticulum (Fig. 1A).

Interestingly, we found that the gene encoding isovaleryl-CoA dehydrogenase was also induced in

N. benthamiana; therefore, acyl sugar biosynthesis may also be competing with catabolic enzymes acting downstream of BCKD for acyl-CoA substrates (Table I). This suggests possibilities for increasing flux to acyl sugar side chains by transgenic manipulation of both enzymatic steps.

Of the BCAA biosynthetic genes up-regulated in trichomes, three were key regulatory steps all subject to feedback inhibition by BCAAs (Binder et al., 2007). TD is the first step for Ile synthesis (up-regulated principally in *S. pennellii* trichomes), ALS governs flux into all BCAAs (up-regulated in *S. pennellii* trichomes), and IPMS is the first committed step for Leu synthesis (up-regulated only in *N. benthamiana* trichomes). Elevation of TD and ALS in *S. pennellii* indicates the importance of keto acid precursor provision for BCFA synthesis in the trichomes and could be indicative of high flux occurring here in wild tomato. Identification of a highly elevated IPMS transcript in *N. benthamiana* trichomes, together with the high ranking of subsequent steps of the Leu biosynthetic pathway (IPMD and IPDS-L) in the microarray analysis for this species, underline the importance of the α-KAE pathway in tobacco species and specifically support isotopic labeling studies showing that this pathway operates in trichomes from *N. benthamiana* (Kroumova and Wagner, 2003). Importantly, we found no evidence for up-regulation of *IPMS* genes in *S. pennellii*, where elongation of acyl sugar chains is thought to occur by FAS. In *N. benthamiana*, extended cycling of α-KAE, as proposed, generates the majority of acyl sugar chains (*iso* and *anteiso* branched C_8), whereas for *S. pennellii*, this pathway likely provides just one minor component (3MeC4:0) with only one cycle of α-KAE required (Fig. 1). Further work is required to determine if any of the above trichome-expressed enzymes of BCAA synthesis have tailored substrate specificities and feedback controls that meet the differing requirements in the two species.

Overall, the similarities in gene regulation in BCAA metabolism typified by BCKD point toward common mechanisms for transcriptional control in trichomes from the two species. Some divergence is indicated by the existence of species-specific trichome-expressed enzyme isoforms of α-KAE, supporting distinct elongation mechanisms and distinct acyl sugar compositions.

Photosynthesis in Acyl Sugar-Producing Trichomes

In addition to the induction of BCAA production and breakdown, we observed down-regulation in the trichomes of genes associated with photosynthesis. This was consistent with our observations of low levels of chlorophyll in trichome preparations and indicated that photosynthesis occurs at significantly lower levels in the trichomes than in the rest of the leaf as a whole in *S. pennellii* and *N. benthamiana*. It is difficult to rule out whether some of the chlorophyll originates from low levels of contamination of trichome harvests with photosynthetic cell types. Despite this caveat, some trichomes (and most guard cells) are known to be capable of photosynthesis, although epidermal pavement cells are generally nonphotosynthetic. Detached tobacco trichome heads, in particular, have been shown to have the ability to produce terpenoids and acyl sugars from CO_2 (Kandra and Wagner, 1988). Nevertheless, feeding studies with epidermal peels indicate that tobacco trichomes are also capable of receiving imported Suc for this purpose (and do so more avidly than with labeled Glc or acetate; Kandra and Wagner, 1988). It is not known if *S. pennellii* tomato glandular trichomes are photosynthetically competent, but chlorophyll-containing plastids have been identified in the major trichome types in cultivated tomato (Pike and Howells, 2002). As acyl sugar accumulation can reach very high levels in *S. pennellii* and in some tobacco species (Fobes et al., 1985; Wagner, 1991), it is likely that trichomes import at least some proportion of the photosynthates they need for acyl sugar production from other leaf tissues.

Involvement of FAS in BCFA Elongation and Its Association with a Compensatory Mechanism That Maintains Exudate Output

The results of isotopic labeling studies suggested that BCFAs are elongated in two carbon steps in *S. pennellii* and *D. metel* trichomes (van der Hoeven and Steffens, 2000; Kroumova and Wagner, 2003). Similar studies indicate α-KAE for short branched-chain production in tobacco and *Petunia* acyl sugars (Kroumova and Wagner 2003). FAS elongation appears to be employed for branched-chain wax components in tobacco species, however (Kaneda, 1967; Kolattukudy, 1968; Kroumova and Wagner, 1999).

Despite the evidence for FAS in branched-chain elongation, few genes associated with FAS were identified in the microarray analysis as highly trichome expressed. The operation of this pathway was tested by application of the KAS I/II inhibitor cerulenin to the leaves of *S. pennellii* plants. This led to the reduction of both SCFAs and BCFAs of C_{10} and over by 50% in exudates. The role of KAS genes was tested further by gene knockdown in *S. pennellii*. Three genes encoding KAS I enzymes were identified in tomato EST collections. The predicted products of *KAS IA* and *KAS IB* cluster with other plant KAS I proteins, whereas KAS IC appears to be more divergent (data not shown). While silencing *KAS IC* did not have a significant effect on fatty acid composition, down-regulation of both *KAS IA* and *KAS IB* caused a reduction in 8MeC9:0 output. This silencing phenotype suggests that both enzymes are required for normal BCFA production in the trichomes. Taken together, these data suggest the involvement of plastid FAS in BCFA elongation (Fig. 1A).

Surprisingly, in both cases the decrease in BCFA production was associated with an increase in the accumulation of the SCFAs C10:0 and C12:0 into

acyl sugars. This was reflected in an increase in trichome straight-chain to branched-chain acyl-CoAs of C_{10} to C_{12}. A similar compensatory effect was also observed in the BCKD knockdown experiments, notably with *S. pennellii* acyl sugars and *N. benthamiana* wax alkanes. Taken together, these data suggest that reducing branched-chain precursor supply for FAS-mediated branched-chain elongation can result in a compensatory up-regulation with straight chains. One possibility is that branched-chain and straight-chain elongation pathways utilizing FAS could be competing for the same malonyl (-CoA or -acyl-carrier protein) pools. Given that the compensatory effect was observed with *S. pennellii* knockdowns of individual *KAS IA* and *IB* genes but not with the cerulenin treatment, it follows that other cerulenin-sensitive KAS genes might be involved in straight-chain production. Further experiments are required to determine if regulatory feedback mechanisms are involved.

CONCLUSION

Our genomic study has identified key genes potentially relevant to acyl sugar synthesis and subject to transcriptional control in trichomes in Solanaceae (using the models *S. pennellii* and *N. benthamiana*). Functional analysis via gene knockdown was carried out comprehensively for the first dedicated step of BCAA breakdown undertaken by the BCKD complex. Knockdown of BCKD demonstrated that this complex is required for branched-chain production for both acyl sugars and wax alkanes. Gene expression studies supported the operation of the α-KAE pathway in tobacco but did not support this in tomato for acyl sugar branched-chain synthesis. Inhibitor feeding and *KAS I* gene knockdowns verified the importance of FAS in *S. pennellii*. Gene knockdowns of *BCKD* and *KAS I* revealed compensatory mechanisms for FAS-mediated elongation of acyl sugar and wax alkane chains that appear to maintain constant exudate output.

Fully testing the current models of branched-chain production will require the determination of substrate specificities and intracellular locations for the various enzymes combined with overexpression studies in planta.

MATERIALS AND METHODS

Plant Material

Nicotiana benthamiana seeds were germinated directly onto soil (Levingtons) in 8-cm pots, and all experiments were carried out under greenhouse conditions with supplemental lighting providing a minimum illumination period of 14 h (4 h in winter, 70 μE; 20°C–24°C day, 16°C night). *Solanum pennellii* (LA0716) was originally obtained from the CM Rick Tomato Genetics Resource Center (University of California, Davis). Seeds were routinely collected from mature fruit (indicated by fruit softening), dried in sand for 1 week, and sterilized by soaking in 10% (w/v) trisodium phosphate dodecahydrate (30 min at room temperature) and then for 2 h in fresh solution. Seeds were then washed five times in sterile water, incubated at 50°C in water (30 min), placed in 2.7% sodium hypochlorite (30 min), washed five times in sterile water, and placed in soil (Levingtons) to germinate in the above greenhouse conditions. VIGS experiments on *S. pennellii* were carried out in a growth room under cycles of 16 h of light (20°C, 150 μE) and 8 h of dark (18°C). Leaf trichomes were counted with a microscope after staining with Sudan Red 7B according to a published protocol (Brundrett et al., 1991). Square leaf segments (approximately 5 mm^2) were placed for 1 h, adaxial side down, onto a polyethylene glycol-400 solution containing 0.1% (w/v) Sudan Red (*S. pennellii*) or a 45% (v/v) glycerol/50% (v/v) polyethylene glycol-400 solution containing 0.05% (w/v) of the same dye (*N. benthamiana*).

Leaf trichomes were harvested from leaf material essentially according to Wang et al. (2001). Leaves frozen in liquid nitrogen were brushed on both sides (using a flat 5-mm-wide synthetic fiber paintbrush), and leaf fragments were removed from trichomes by filtration through a 0.5-mm steel mesh test filter (Endecotts). Stem trichomes were harvested by collecting stems immersed in liquid nitrogen and vortexing frozen stems together in disposable centrifuge tubes for 20 s.

Metabolite Profiling

Leaf exudates were harvested by briefly washing young expanded leaves in methanol. In the case of *N. benthamiana*, leaves were washed in a 2.5-mL methanol solution containing 37.5 μg of Suc monolaurate (Sigma-Aldrich) added as an internal standard. For the analysis of acyl sugar or fatty acid content, the third and fourth leaves (*N. benthamiana*) or leaflets (*S. pennellii*; approximately 2–4 cm in length) counting from the apex were typically used. Data are expressed on a fresh weight basis except when comparing different sized leaves, in which case surface area is the preferred reference parameter. It was found that the mass-to-surface area ratio was similar in treatments versus controls for the experiments described.

Acyl sugars were resolved by injection of 20 μL of methanolic extract (300 ng of ISTD) onto a porous graphite carbon column (Hypercarb; Thermo Hypersil) for LC-MS analysis. HPLC separation was achieved from samples held at 8°C in a AS3000 autosampler (Thermo Separation Products) using a ternary gradient generated by a P4000 pump (Thermo Separation Products) with solvents A (acetonitrile), B (water), and C (tetrahydrofuran), where all solvents contained 0.2% formic acid. Compounds were eluted by the following stepwise linear gradient program at 0.4 mL min^{-1}: 0 to 1 min, isocratic 50% A and 50% B; 1 to 15 min, to 60% A and 40% B; 15 to 50 min, to 40% A and 60% C, hold until 55 min; 55 to 55.1 min, to initial conditions, then hold until 60 min. The column was maintained at 30°C throughout the run. Column flow was directed through an atmospheric chemical ionization source attached to an LCQ mass spectrometer (Thermo). Source conditions were as follows: atmospheric chemical ionization source vaporizer temperature, 500°C; sheath gas flow, 60 units; auxiliary gas flow, 20 units; source current, 5 μA (positive mode); capillary voltage, 15 V; no tube lens offset was used. The LCQ mass spectrometer was operated in data-dependent MS2 mode (isolation width, 4 mass-to-charge ratio; normalized collision energy, 35%; dynamic exclusion enabled), with full-scan mass spectra collected in the 50 to 1,000 mass-to-charge ratio range (extracted ion masses were used for quantification) and MS2 spectra used for structural analyses. The proposed fragmentation pathway for the predictive compositional analysis of acyl chain length and carbohydrate backbone is shown in Supplemental Figure S3. Major acyl sugar peaks were also collected after HPLC separation, dried in a Speedivac, and subjected to fatty acid methyl esters (FAMES) analysis by GC-FID (see below) for compositional identification. Acyl sugar amounts were calculated relative to the internal standard, assuming a response ratio of 1 for unknowns.

For GC-FID analysis of FAMES, *N. benthamiana* methanol extracts (containing 15 ng μL^{-1} Suc monolaurate) were dried down in a SpeedVac (Savant), redissolved in 500 μL of 0.1 M sodium methoxide, and incubated for 20 min at room temperature. Following the addition of 0.25 mL of 0.9% (w/v) KCl, methyl esters were partitioned into 200 μL of hexane. In the case of *S. pennellii*, the leaves were washed in a methanolic solution containing 50 ng μL^{-1} heptanoic acid methyl ester (Larodan) as an internal standard. The resulting extracts (approximately 1.5 mL) were subjected to transmethylation for 2 h at room temperature by addition of 37.5 μL of 8 M NaOH. After neutralization by addition of 375 μL of 1 N HCl, the methyl esters were partitioned into 200 μL of hexane, and 1 μL was analyzed by GC-FID. This analysis was performed with a GC Ultra (Thermo) system fitted with a 10 m × 0.1 mm i.d. × 0.2 μm phase thickness BPX70 capillary column (SGE). The column was operated with H_2 as carrier gas in programmed flow mode under the following conditions: 0 to 0.1

min, 0.2 mL min^{-1}; increase at 5 mL min^{-1} min^{-1} to 0.5 mL min^{-1} for the remainder of the run. Samples were injected into the liner held at 230°C at a split ratio of 150:1. The oven was temperature programmed as follows: 40°C hold for 1 min; increase at 16°C min^{-1} to 220°C.

Acyl-CoA analysis was carried out on 10 mg of fresh leaf, stem, or harvested trichome material that was first pulverized in liquid nitrogen. Separation procedures and preparation of standards were followed as described by Ishizaki et al. (2005). Acyl-CoA chains of C10:0 and over were separated with a LUNA 150 × 2 mm C18(2) column (Phenomenex), and shorter chains were separated with a Hypercarb 100 × 3 mm porous graphitic carbon column (Thermo Hypersil) as described.

Wax analysis was carried out according to Broun et al. (2004). Branched-chain alkanes in gas chromatography-mass spectrometry traces were identified according to Kaneda (1967).

Measurement of Gene Expression

Semiquantitative RT-PCR was carried out using 300 ng of RNA for the RT reaction with SuperScript II (Invitrogen) followed by touch-down PCR with Ex-Taq DNA polymerase (Takara) according to the manufacturer's instructions using primers with melting temperatures of 50°C. PCR products were examined by ethidium bromide-DNA gel electrophoresis after two different cycling times per gene primer set, and results were verified with duplicate tissue isolations in all cases. Real-time RT-PCR was carried out on RT reactions (see above) using PowerSybr Green PCR Master Mix (Applied Biosystems) with an ABI Prism 7000 Sequence Vector System (Applied Biosystems) and primers with melting temperatures of 60°C (Supplemental Table S6). Cycling parameters were 95°C for 15 s, 60°C for 1 min, and 72°C for 30 s. Primers were designed using Prime-it III software (Rozen and Skaletsky, 2000), and data were processed using Sequence Detection Software (Applied Biosystems). Gene expression ratios were calculated in Microsoft Excel for two given tissues or conditions using the comparative threshold method, normalizing with actin primers (Livak and Schmittgen, 2001). If primer efficiencies differed by more than 5% from those of the actin primers (Supplemental Table S6), the relative standard method was employed (Pfaffl, 2001).

Microarray Analysis

RNA for the microarray was obtained from leaf trichomes and leaves from which trichomes had been removed, from replicate pools of 5-week-old plants grown as above, and gene expression was compared between the two samples. Chlorophyll was quantified according to Porra et al. (1989). Tomato TOM2 long oligonucleotide arrays representing 12,000 unigene sequences were probed simultaneously with Cy5- and Cy3-labeled probes. Probe preparation, hybridization conditions, and the washing protocol were as described previously (Alba et al., 2004). Microarray images were analyzed to generate numerical data using ImaGene software (version 5.5; BioDiscovery). Spots flagged by ImaGene as poor quality and spots with mean signal intensities less than local background intensities plus 2 SDs of the local background in both channels were not included in the downstream statistical analysis. A print-tip Lowess normalization strategy was applied to normalize the ratio values for each array using the marray package in Bioconductor (Yang et al., 2002). Differentially expressed genes were identified using Patterns from Gene Expression (Grant et al., 2005). Genes with false discovery rates of less than 0.1 (*S. pennellii*) and 0.05 (*N. benthamiana*) and fold change greater than or equal to 2-fold were identified as differentially expressed genes. Functional annotations were assigned according to Alba et al. (2005).

VIGS

Down-regulation of gene expression was carried out using the tobacco rattle virus RNA2-based VIGS vector pTRV2 (pYL156; Liu et al., 2002b). Typically, 400- to 600-bp gene fragments were amplified by PCR using primers containing *Xho*I (5′) and *Bam*HI (3′) restriction sites (Supplemental Table S6) and cloned, in the antisense orientation, into the pTRV2 vector.

VIGS was carried out according to a published protocol (Liu et al., 2002a) using *Agrobacterium tumefaciens* GV3101 strains carrying TRV2 and TRV1 binary vectors. In the case of *N. benthamiana*, *Agrobacterium* cells from 5-mL overnight cultures were collected by centrifugation and resuspended in an equal volume of infiltration medium (10 mM $MgCl_2$ and 100 μm acetosyringone). After 2 h of incubation at room temperature, *Agrobacterium* suspensions containing TRV1 or TRV2 binary vectors were mixed in a 1:100 ratio. For silencing experiments, leaves of plants at the four-leaf stage were infiltrated with the mixed suspension using a 2-mL syringe, and infected plants were grown under greenhouse conditions for another 5 weeks before analysis. In the case of *S. pennellii*, 5-mL saturated *Agrobacterium* cultures were added to 50 mL of Luria-Bertani medium containing 10 mM MES (pH 5.5) and 20 μm acetosyringone and grown overnight. The cells were collected by centrifugation, resuspended in an equal volume of 10 mM $MgCl_2$, then harvested again and resuspended in 5 mL of infiltration medium (10 mM MES [pH 5.5], 10 mM $MgCl_2$, and 200 μM acetosyringone). After a 2-h incubation at room temperature, TRV1 and TRV2 *Agrobacterium* suspensions were mixed 1:1 and diluted to a final optical density at 600 nm of about 0.4 in about 200 mL of infiltration medium. The mixed suspension was then used to vacuum infiltrate seedlings at the first true leaf stage (leaf size approximately 5 mm) for 2 min. Infected plants were placed in a growth room (see above) and analyzed 5 to 6 weeks later. A pTRV2-PDS construct containing a 1,545-bp tomato genomic sequence encoding PDS (S. Ekengren, personal communication) was used as a positive control to assess the extent of VIGS.

Inhibitor Studies

The third or fourth leaf relative to the apex (typically bearing five to seven leaflets of 2–3 cm length) was harvested from mature greenhouse-grown plants to generate cuttings. These were dipped for 2 to 3 s in 100% ethanol to remove exuded acyl sugars and rapidly transferred to water to wash off ethanol. The cuttings were then briefly blotted dry, placed into shallow foil-covered trays containing 50 mL of inhibitor or control solution, and placed under greenhouse conditions. Cerulenin (Sigma-Aldrich) was first dissolved in acetone at 10 mg mL^{-1} and then added to water to produce the 100 μM solutions used in inhibitor experiments.

Sequence data for *N. benthamiana* stem trichome ESTs (1–6,995) can be found in the GenBank/EMBL data libraries under accession numbers ES884240 to ES890108 and EX533310 to EX534435.

Supplemental Data

The following materials are available in the online version of this article.

Supplemental Figure S1. LC-MS trace of *N. benthamiana* leaf exudate separation.

Supplemental Figure S2. Yield comparison of different acyl sugar extraction conditions.

Supplemental Figure S3. Structural analysis and fragmentation patterns of acyl sugars.

Supplemental Figure S4. Developmental profiles of leaf exudates.

Supplemental Figure S5. De novo production of acyl sugars after removal from leaf.

Supplemental Figure S6. *KAS* gene expression survey in *S. pennellii* tissues.

Supplemental Table S1. Acyl sugar composition of *N. benthamiana* leaf exudate.

Supplemental Table S2. *N. benthamiana* genes differentially expressed in trichomes.

Supplemental Table S3. *S. pennellii* genes differentially expressed in trichomes.

Supplemental Table S4. Differentially expressed genes common to both species.

Supplemental Table S5. Chlorophyll measurements in trichomes.

Supplemental Table S6. List of primers.

Supplemental Table S7. Gene accession numbers.

ACKNOWLEDGMENTS

We thank Dr. Dinesh Kumar for providing TRV1 and TRV2 binary vectors and Dr. Sophia Ekengren for providing the pTRV2-LePDS construct used in VIGS experiments. We are grateful to Dave Harvey and Stuart Graham for assistance with metabolite profiling and to Dr. Andy King for discussions on real-time RT-PCR. We thank Dr. Li Tian for EST plasmid DNA preparation and Ann Harris for EST sequencing.

Received September 7, 2008; accepted October 13, 2008; published October 17, 2008.

LITERATURE CITED

Alba R, Fei Z, Payton P, Liu Y, Moore S, Debbie P, Gordon J, Rose J, Martin G, Tanksley S, et al (2004) ESTs, cDNA microarrays and gene expression profiling: tools for dissecting plant physiology and development. Plant J **39:** 697–714

Alba R, Payton P, Fei Z, McQuinn R, Debbie P, Martin G, Tanksley S, Giovannoni J (2005) Transcriptome and selected fruit metabolite analysis reveal multiple points of ethylene regulatory control during tomato fruit development. Plant Cell **17:** 2954–2965

Arrendale RF, Severson RF, Sisson VA, Costello CE, Leary JA, Himmelsbach DS, van Halbeek H (1990) Characterization of the sucrose ester fraction from *Nicotiana glutinosa*. J Agric Food Chem **38:** 75–85

Aziz N, Paiva NL, May GD, Dixon RA (2005) Transcriptome analysis of alfalfa glandular trichomes. Planta **221:** 28–38

Beisson F, Koo AJ, Ruuska S, Schwender J, Pollard M, Thelen JJ, Paddock T, Salas JJ, Savage L, Milcamps A, et al (2003) Census of the candidates, a study of the distribution of expressed sequence tags in organs, and a Web-based database. Plant Physiol **132:** 681–697

Binder S, Knill T, Schuster J (2007) Branched-chain amino acid metabolism in higher plants. Physiol Plant **129:** 68–78

Bonierbale MW, Plaisted RL, Pineda O, Tanksley SD (1994) QTL analysis of trichome-mediated insect resistance in potato. Theor Appl Genet **87:** 973–987

Broun P, Poindexter P, Osborne E, Jiang CZ, Riechmann JL (2004) WIN1, a transcriptional activator of epidermal wax accumulation in Arabidopsis. Proc Natl Acad Sci USA **101:** 4706–4711

Brundrett MC, Kendrick B, Peterson CA (1991) Efficient lipid staining in plant material with Sudan red 7B or fluorol yellow 088 in polyethylene glycol-glycerol. Biotech Histochem **66:** 111–116

Burke BA, Goldsby G, Mudd JB (1987) Polar epicuticular lipids of Lycopersicon pennellii. Phytochemistry **26:** 2567–2571

Chortyk OT (1997) Characterization of insecticidal sugar esters of Petunia. J Agric Food Chem **45:** 270–275

Chortyk OT, Severson RF, Cutler HC, Sisson VA (1993) Antibiotic activities of sugar esters isolated from selected *Nicotiana* species. Biosci Biotechnol Biochem **57:** 1355–1356

de Kraker JW, Luck K, Textor S, Tokuhisa JG, Gershenzon J (2007) Two Arabidopsis genes (IPMS1 and IPMS2) encode isopropylmalate synthase, the branchpoint step in the biosynthesis of leucine. Plant Physiol **143:** 970–986

Ding L, Xie F, Zhao M, Xie J, Xu G (2006) Rapid characterization of the sucrose esters from oriental tobacco using liquid chromatography/ion trap mass spectrometry. Rapid Commun Mass Spectrom **20:** 2816–2822

Field B, Furniss C, Wilkinson A, Mithen R (2006) Expression of a Brassica isopropylmalate synthase gene in Arabidopsis perturbs both glucosinolate and amino acid metabolism. Plant Mol Biol **60:** 717–727

Fobes JF, Mudd JB, Marsden MPF (1985) Epicuticular lipid accumulation on the leaves of *Lycopersicon pennellii* (Corr.) D'Arcy and *Lycopersicon esculentum* Mill. Plant Physiol **77:** 567–570

Gang DR, Wang J, Dudareva N, Nam KH, Simon JE, Lewinsohn E, Pichersky E (2001) An investigation of the storage and biosynthesis of phenylpropenes in sweet basil. Plant Physiol **125:** 539–555

Ghangas GS, Steffens JC (1995) 1-O-Acyl-beta-D-glucoses as fatty acid donors in transacylation reactions. Arch Biochem Biophys **316:** 370–377

Goffreda JC, Szymkowiak EJ, Sussex IM, Mutschler MA (1990) Chimeric tomato plants show that aphid resistance and triacylglucose production are epidermal autonomous characters. Plant Cell **2:** 643–649

Grant GR, Liu J, Stoeckert CJ Jr (2005) A practical false discovery rate approach to identifying patterns of differential expression in microarray data. Bioinformatics **11:** 2684–2690

Hill K, Rhode O (1999) Sugar-based surfactants for consumer products and technical applications. Fett Lipid **101:** 25–33

Ishizaki K, Larson TR, Schauer N, Fernie AR, Graham IA, Leaver CJ (2005) The critical role of *Arabidopsis* electron-transfer flavoprotein: ubiquinone oxidoreductase during dark-induced starvation. Plant Cell **9:** 2587–2600

Kandra L, Severson R, Wagner GJ (1990) Modified branched-chain amino acid pathways give rise to acyl acids of sucrose esters exuded from tobacco leaf trichomes. Eur J Biochem **188:** 385–391

Kandra L, Wagner GJ (1988) Studies of the site and mode of biosynthesis of tobacco trichome exudate components. Arch Biochem Biophys **265:** 425–432

Kandra L, Wagner GJ (1990) Chlorsulfuron modifies biosynthesis of acyl acid substituents of sucrose esters secreted by tobacco trichomes. Plant Physiol **94:** 906–912

Kaneda T (1967) Biosynthesis of long-chain hydrocarbons. I. Incorporation of L-valine, L-threonine, L-isoleucine, and L-leucine into specific branched-chain hydrocarbons in tobacco. Biochemistry **6:** 2023–2031

King RR, Calhoun LA (1988) 2,3-Di-O- and 1,2,3-tri-O-acylated glucose esters from the glandular trichomes of *Datura metel*. Phytochemistry **27:** 3761–3763

King RR, Calhoun LA, Singh RP, Boucher A (1990) Sucrose esters associated with glandular trichomes of wild *Lycopersicon* species. Phytochemistry **29:** 2115–2118

Kolattukudy PE (1968) Further evidence for an elongation-decarboxylation mechanism in the biosynthesis of paraffins in leaves. Plant Physiol **43:** 375–383

Koo AJ, Fulda M, Browse J, Ohlrogge JB (2005) Identification of a plastid acyl-acyl carrier protein synthetase in Arabidopsis and its role in the activation and elongation of exogenous fatty acids. Plant J **44:** 620–632

Kroumova AB, Wagner GJ (1999) Mechanisms for elongation in the biosynthesis of fatty acid components of epi-cuticular waxes. Phytochemistry **50:** 1341–1345

Kroumova AB, Wagner GJ (2003) Different elongation pathways in the biosynthesis of acyl groups of trichome exudate sugar esters from various solanaceous plants. Planta **216:** 1013–1021

Kroumova AB, Zie Z, Wagner GJ (1994) A pathway for the biosynthesis of straight and branched, odd- and even-length, medium-chain fatty acids in plants. Proc Natl Acad Sci USA **91:** 11437–11441

Kuai JP, Ghangas GS, Steffens JC (1997) Regulation of triacylglucose fatty acid composition (uridine diphosphate glucose:fatty acid glucosyltransferases with overlapping chains-length specificity). Plant Physiol **115:** 1581–1587

Lange BM, Wildung MR, Stauber EJ, Sanchez C, Pouchnik D, Croteau R (2000) Probing essential oil biosynthesis and secretion by functional evaluation of expressed sequence tags from mint glandular trichomes. Proc Natl Acad Sci USA **97:** 2934–2939

Lawson DM, Lunde CF, Mutschler MA (1997) Marker-assisted transfer of acyl sugar-mediated pest resistance from the wild tomato, *Lycopersicon pennellii*, to the cultivated tomato, *Lycopersicon esculentum*. Mol Breed **3:** 307–317

Li AX, Eannetta N, Ghangas GS, Steffens JC (1999) Glucose polyester biosynthesis: purification and characterization of a glucose acyltransferase. Plant Physiol **121:** 453–460

Li AX, Steffens JC (2000) An acyltransferase catalyzing the formation of diacylglucose is a serine carboxypeptidase-like protein. Proc Natl Acad Sci USA **97:** 6902–6907

Liu Y, Schiff M, Dinesh-Kumar SP (2002a) Virus-induced gene silencing in tomato. Plant J **31:** 777–786

Liu Y, Schiff M, Marathe R, Dinesh-Kumar SP (2002b) Tobacco Rar1, EDS1 and NPR1/NIM1 like genes are required for N-mediated resistance to tobacco mosaic virus. Plant J **30:** 415–429

Livak KJ, Schmittgen TD (2001) Analysis of relative gene expression data using real-time quantitative PCR and the 2-DDCT method. Methods **25:** 402–408

Luckwill LC (1943) The genus *Lycopersicon*. Aberdeen University Studies **120:** 5–44

McKenzie CL, Weathersbee AA III, Puterka GJ (2005) Toxicity of sucrose octanoate to egg, nymphal adult *Bemisia tabaci* (Hemiptera: Aleyrodidae) using a novel plant-based bioassay. J Econ Entomol **98:** 1242–1247

Mooney BP, Miernyk JA, Randall DD (2002) The complex fate of alpha-ketoacids. Annu Rev Plant Biol **53:** 357–375

Mutschler MA, Wally AM, Rojas K, Cobb E (2001) Transferal of acyl sugar-

mediated multiple pest resistance to cultivated tomato. HortScience **36:** 492

Ohya I, Sinozaki Y, Tobita T, Takahashi H, Matsuzaki T, Koiwai A (1994) Sucrose esters from the surface lipids of *Nicotiana cavicola*. Phytochemistry **37:** 143–145

Pfaffl MW (2001) A new mathematical model for relative quantification in real-time RT-PCR. Nucleic Acids Res **29:** E45

Pike KA, Howells CA (2002) Plastid and stromule morphogenesis in tomato. Ann Bot (Lond) **90:** 559–566

Porra RJ, Thompson WA, Kriedemann PE (1989) Determination of accurate extinction coefficients and simultaneous equations for assaying chlorophylls a and b extracted with four different solvents: verification of the concentration of chlorophyll standards by atomic absorption spectrometry. Biochim Biophys Acta **975:** 384–394

Puterka GJ, Farone W, Palmer T, Barrington A (2003) Structure-function relationships affecting the insecticidal and miticidal activity of sugar esters. J Econ Entomol **96:** 636–644

Rensink WA, Lee Y, Liu J, Iobst S, Ouyang S, Buell CR (2005) Comparative analyses of six solanaceous transcriptomes reveal a high degree of sequence conservation and species-specific transcripts. BMC Genomics **6:** 124

Rozen S, Skaletsky HJ (2000) Primer3 on the WWW for general users and for biologist programmers. *In* S Krawetz, S Misener, eds, Bioinformatics Methods and Protocols: Methods in Molecular Biology. Humana Press, Totowa, NJ, pp 365–386

Severson RF, Arrendale RF, Chortyk OT, Green CR, Thome FA, Stewart JL, Johnson AW (1985) Isolation and characterization of the sucrose esters of the cuticular waxes of green tobacco leaf. J Agric Food Chem **33:** 870–875

Shapiro JA, Steffens JC, Mutschler MA (1994) Acyl sugars of the wild tomato *Lycopersicon pennellii* in relation to geographic distribution of the species. Biochem Syst Ecol **22:** 545–561

Shinozaki Y, Matsuzaki T, Suhara S, Tobita T, Shigematsu H, Koiwai A (1991) New types of glycolipids from the surface lipids of Nicotiana umbratica. Agric Biol Chem **55:** 751–756

Taylor NL, Heazlewood JL, Day DA, Millar AH (2004) Lipoic acid-dependent oxidative catabolism of alpha-keto acids in mitochondria provides evidence for branched-chain amino acid catabolism in Arabidopsis. Plant Physiol **134:** 838–848

van der Hoeven RS, Steffens JC (2000) Biosynthesis and elongation of short- and medium-chain-length fatty acids. Plant Physiol **122:** 275–282

Wagner GJ (1991) Secreting glandular trichomes: more than just hairs. Plant Physiol **96:** 675–679

Walters DS, Steffens JC (1990) Branched chain amino acid metabolism in the biosynthesis of *Lycopersicon pennellii* glucose esters. Plant Physiol **93:** 1544–1551

Wang E, Wang R, deParasis J, Loughrin JH, Gan S, Wagner GJ (2001) Suppression of a P450 hydroxylase gene in plant trichome glands enhances natural-product-based aphid resistance. Nat Biotechnol **19:** 371–374

Yang YH, Dudoit S, Luu P, Lin DM, Peng V, Ngai J, Speed TP (2002) Normalization for cDNA microarray data: a robust composite method addressing single and multiple slide systematic variation. Nucleic Acids Res **30:** e15

Yasuno R, von Wettstein-Knowles P, Wada H (2004) Identification and molecular characterization of the beta-ketoacyl-[acyl carrier protein] synthase component of the Arabidopsis mitochondrial fatty acid synthase. J Biol Chem **279:** 8242–8251